RSC Advances

PAPER

View Article Online
View Journal | View Issue

Cite this: *RSC Adv.*, 2025, **15**, 31230

Combined flotation-oxygen pressure leaching process for treatment of copper smelting slag with a high oxidation rate and its kinetic study

Zixuan Yang,[a] Yuanlin Ma,[b] Shuting Wang[a] and Tingtao Bi *[a]

A process route combining flotation for recovering easily floatable sulfide copper minerals and oxygen pressure acid leaching (OPAL) was employed to comprehensively recover valuable metals (Cu, Mo, Fe, *etc.*) from copper smelting slag with a high oxidation degree. The oxidative leaching process selectively dissolved and recovered Cu and Mo while transforming Fe into leach residue, rendering it suitable as a raw material for iron and steel smelting. Under optimal conditions, the leaching recoveries for Cu and Mo reached 96.87% and 95.39%, respectively, with over 90% of Fe in the residue phase. Kinetic studies revealed that the OPAL process conforms to the shrinking core model without a solid product layer. The leaching rate was initially controlled by the chemical reaction, transitioned to mixed control during the intermediate stage, and was finally governed by diffusion through the solid product layer in the later stage. Based on this, the kinetic equations for Cu and Mo leaching during the chemically controlled stage were fitted and calculated, and the reaction model was established.

Received 9th April 2025
Accepted 31st July 2025

DOI: 10.1039/d5ra02448j

rsc.li/rsc-advances

1 Introduction

Copper (Cu), an indispensable fundamental raw material in modern industry and socio-economic development, is widely utilized in electrical appliances, transportation, light industry, machinery, construction, and defense industries due to its excellent physicochemical properties.[1,2] Its metallic form and alloys have become essential materials for modern industry, agriculture, national defense, and scientific technologies.[3] Copper smelting slag is generated during the pyrometallurgical processing of copper concentrates (with a grade of >20%) into high-purity copper metal. Current copper smelting slags typically contain over 0.5% copper, significantly exceeding the average grade of most copper ores. These slags are rich in valuable metals, such as Cu, Fe, Zn, and Mo, yet their complex composition, dense structure, and hardened texture make the recovery of copper, iron, and other resources extremely challenging.[4,5] Globally, vast quantities of copper smelting slag are produced annually, with China alone generating approximately 20 million metric tons each year.[6] To date, the total amount of copper smelting slag has reached 150 million metric tons, primarily in the form of slow-cooled slag and water-quenched slag. The massive stockpiling of copper smelting slag not only occupies land resources but also poses severe environmental risks.[7] The slag contains non-biodegradable toxic substances, such as arsenic and lead, which can infiltrate soil, contaminate water systems, and bioaccumulate in organisms, leading to chronic health hazards and diseases. In order to make rational use of copper smelting slag, relieve the pressure on mineral resources and achieve a win–win situation for the economy and environment, it is imperative to strengthen the resource utilization and eco-friendly treatment of copper smelting slag.[8–10]

In recent years, advancements in copper smelting technologies and the increasing scarcity of copper concentrate raw materials have driven significant progress in the comprehensive utilization and recycling of copper smelting slag. Current recovery processes primarily include mineral processing and metallurgical methods. Mineral processing, featuring a simplified flowsheet and lower operational costs, has been widely applied in the mining industry for treating high-sulfur copper smelting slag.[11] Based on differences in hydrophilicity, magnetism, density, and other properties among various valuable metal-bearing phases in the slag, methods such as flotation, magnetic separation, and gravity separation are employed to separate and concentrate target components. Research by Carranza indicates that copper smelting slag contains strongly magnetic components, such as magnetite, alongside non-magnetic components like copper. Given that the copper matte phase is readily captured by flotation reagents, a combined flotation–magnetic separation process can be employed to treat copper smelting slag, following crushing and liberation. Applying this flotation-magnetic separation process to copper smelting slag enables the recovery of up to 80% of the contained copper as concentrate, with the mass fraction of copper matte in the resulting concentrate exceeding 20%.[12] However, it is crucial to note that flotation reagents are

[a]*Yunnan Academy of Ecological and Environmental Sciences, Kunming 650034, China*
[b]*School of Land and Resources Engineering, Kunming University of Science and Technology, Kunming 650093, China*

primarily effective only for the matte phase, while magnetic separation is suitable only for slags where the magnetic properties of the constituent phases differ significantly and the proportion of weakly magnetic fayalite is low. After the beneficiation process, while the copper content is reduced, the phase composition of the tailings remains unchanged from that prior to flotation, resulting in persistent environmental hazards. Metallurgical approaches primarily involve pyrometallurgical reductive roasting and hydrometallurgical leaching to extract valuable metals. During high-temperature oxidative/reductive roasting under molten conditions, copper slag demonstrates enhanced reactivity. Modifying the slag by introducing oxidants, *e.g.*, oxygen, promotes the migration, enrichment, and crystallization of valuable metals, while coarsening grain sizes to facilitate subsequent mineral separation. Although pyrometallurgical methods offer certain advantages, they suffer from high energy consumption, operational complexity, and the generation of environmentally harmful gases such as SO_2 and CO_2. In contrast, hydrometallurgical leaching overcomes the energy-intensive and pollution-related drawbacks of pyrometallurgy, enabling selective extraction of valuable metals. Typically, leaching agents, *e.g.*, sulfuric acid and hydrochloric acid, are mixed with the slag to disrupt the iron silicate lattice structures, liberating encapsulated metals. Subsequent recovery from the leach solutions is achieved *via* solvent extraction or ion exchange.[13,14] Extensive OPAL experiments conducted by Baghalha *et al.* demonstrated that this process enables the highly selective leaching of valuable metals and is suitable for treating slags with structures similar to copper smelting slag. During OPAL, iron ions in the slag undergo a hydrolysis reaction, generating regenerated acid. Consequently, sulfuric acid consumption is only equivalent to one-fifth of the slag weight, significantly lower than that required in atmospheric acid leaching.[15] The OPAL process not only achieves highly selective leaching of valuable metals under conditions of low energy and acid consumption but also effectively addresses issues encountered in atmospheric leaching, such as the co-dissolution of iron and silicon, difficulties in solid–liquid separation, and cumbersome impurity removal procedures.

This study uses the slag with a high oxidation rate generated by a certain copper smelting plant as the research object, and investigates the combined flotation-oxygen pressure leaching process to achieve the comprehensive utilization of valuable metals. It conducts an in-depth study on the leaching kinetics of copper smelting slag in the oxygen pressure sulfuric acid system, clarifies the influencing mechanism of mineral leaching efficiency and the phase reconstruction mechanism of copper, molybdenum, and silicoferrite, and provides a theoretical basis for the harmless and comprehensive utilization of copper smelting slag.

Table 1 Chemical multielement analysis (%)

Element	Cu	Fe	Mo	Zn	SiO_2
Content	2.26	43.95	0.42	1.32	30.51
Element	Ti	Al	K	Ca	S
Content	0.22	2.63	0.58	2.31	0.45

2 Experimental

2.1 Materials

The copper smelting slag used in the experiment was generated at a copper smelting plant in China. A multi-element chemical analysis was carried out on this slag, and the results are shown in Table 1. The copper content in this copper smelting slag is 2.26%, and it contains 43.95% of iron (Fe) and 0.42% of molybdenum (Mo). Simultaneously, a chemical phase analysis of copper in the copper smelting slag was conducted, and the results are shown in Table 2. Among them, the content of free copper oxide is 31.14%, the content of combined copper oxide is 15.35%, and the content of secondary copper sulfide is 48.68%, which belongs to copper smelting slag with a high oxidation rate. X-ray energy dispersive spectroscopy and Mineral Liberation Analysis (MLA) were carried out on cuprite in the copper smelting slag, as shown in Fig. 1. Cuprite (0.31%) occurs as granular particles exhibiting close intergrowth relationships with chalcocite, olivine, silicate mixtures, and magnetite. It predominantly encapsulates chalcocite or is intergrown with olivine, silicate mixtures, and magnetite, with occasional intergrowth observed with cubanite. The dissemination size ranges between 0.01 and 0.3 mm. This mineralogical association results in the encapsulation of copper minerals, making them difficult to concentrate *via* flotation processes.

2.2 Reagents and equipment

2.2.1 Flotation experiment. The original slag sample is ground to achieve a 95% proportion of particles below 0.075 mm. 500 g of the ore sample was added to a flotation machine (model YS-5612, Jilin Prospecting Machinery Co., Ltd, China) for the experiment. The no. 2 oil is used as the frother, butyl xanthate and ammonium dibutyl dithiophosphate as the collectors (industrial grade), and sodium sulfide as the sulfidizing agent (analytical grade). After flotation, the ore sample was dried and weighed, and the prepared samples were used for analysis and detection.

Table 2 Copper phase analysis

Phase	Free copper oxide	Bonded copper oxide	Secondary copper sulfide	Primary copper sulfide	Total copper
Content (%)	0.71	0.35	1.11	0.12	2.28
Distribution rate (%)	31.14	15.35	48.68	5.26	100.00

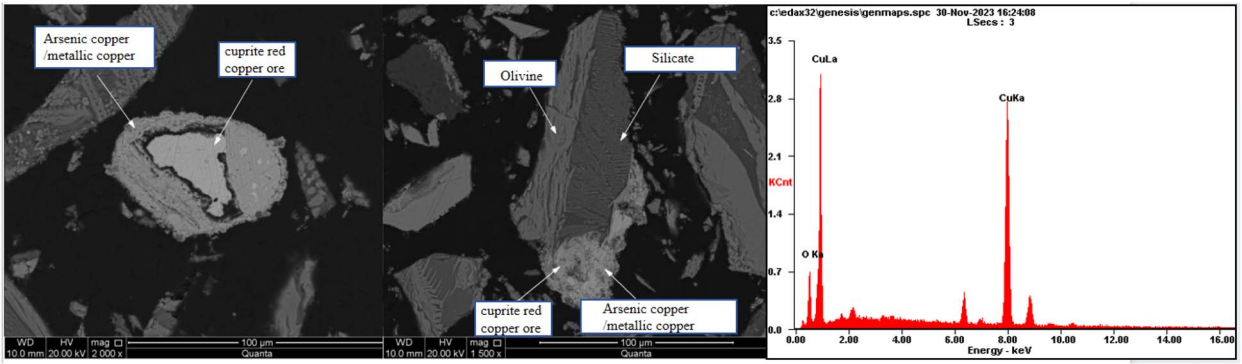

Fig. 1 MLA analysis and X-ray energy spectrum analysis of cuprite in copper smelting slag.

2.2.2 High-pressure leaching experiment. The tailings after flotation were used as the raw material and ground to different finenesses. 200 g of the ore sample was added to a 2 L high-pressure reactor (model: GSH-2L, Weihai Huanyu Chemical Machinery Co., Ltd, China), sulfuric acid (98%) was added, followed by the introduction of oxygen, and different reaction parameters were controlled for oxygen pressure leaching. After the reaction was completed, the sample was filtered, washed three times with pure water, dried, and the prepared samples were used for analysis and detection. The experimental process is shown in Fig. 2.

2.3 Experimental methods

The preliminary process mineralogical analysis revealed that the copper smelting slag has a high oxidation rate, making it difficult to comprehensively recover metals through single flotation. Therefore, flotation was employed to recover the easily separable sulfide minerals, and then oxygen pressure leaching was used to treat the residual metals in the slag.

The tailings after flotation were finely ground in a ball mill and added to a high-pressure reactor. Through single-factor experiments, the effects of different conditions, such as temperature, leaching time, sulfuric acid concentration, oxygen partial pressure, grinding fineness, and liquid-to-solid ratio, on the leaching of copper, molybdenum, and iron in the tailings were investigated respectively. Samples were taken every 10 minutes until the end of the leaching experiment. Based on the experimental results, the kinetic control process was analyzed, and the apparent activation energy of the leaching reaction was calculated.

3 Results and discussion

3.1 Flotation test

Through a large number of preliminary flotation tests, the optimal process condition parameters were ascertained. The flotation process flow and the dosage of reagents are shown in Fig. 3. Butyl xanthate is used as the collector to recover the floatable copper sulfide minerals. Then, sodium sulfide is used as the sulfidizing agent, and a mixture of butyl xanthate and butyl ammonium dibutyl dithiophosphate (1 : 1) is used as the collector to intensively recover some refractory oxidized copper minerals.

In the closed-circuit test, the grade of the produced copper concentrate is 21.54%, and the recovery efficiency is 39.89%. A multi-element analysis of the flotation tailings is carried out, and the specific results are shown in Table 3. As shown in the table, the Cu grade of the tailings after flotation is 0.25% and the Mo content is 0.31%, indicating a high recovery value. The copper phases in the remaining tailings are shown in Table 4. The residual copper is basically mainly free and combined

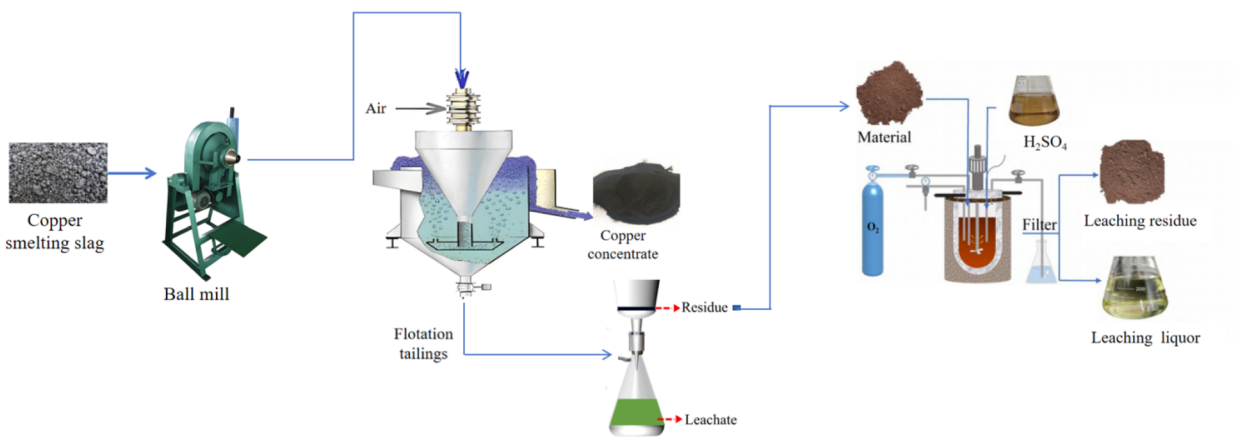

Fig. 2 Combined process of flow of flotation and oxygen pressure leaching.

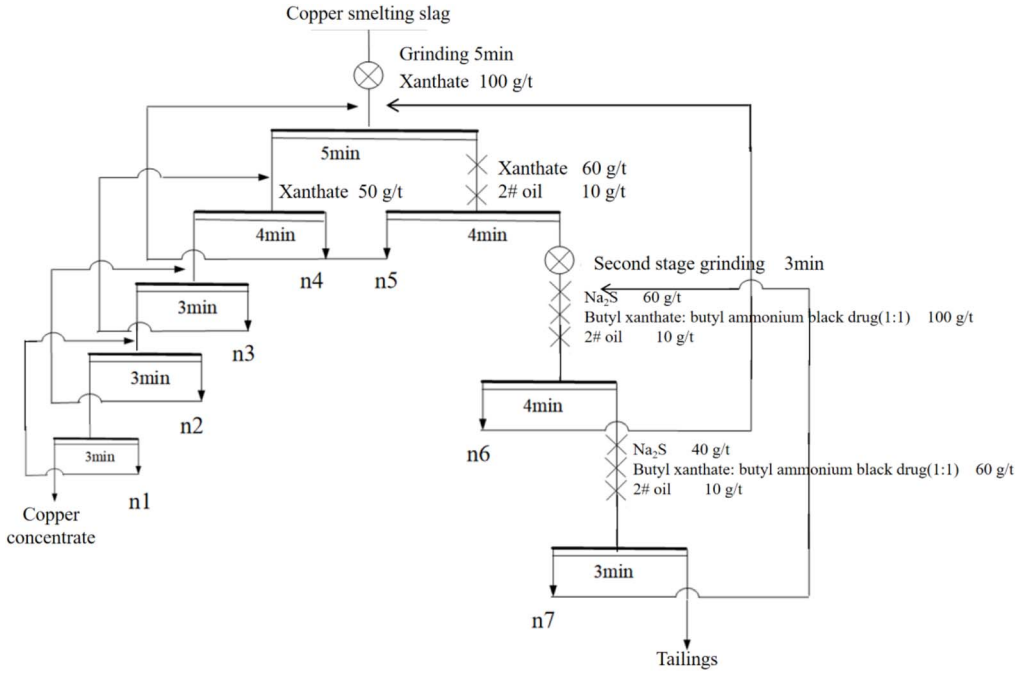

Fig. 3 Flow chart of the closed flotation process.

Table 3 Multi-element analysis of flotation tailings (%)

Element	Cu	Fe	Mo	Zn	SiO_2
Content	0.25	43.95	0.31	1.32	32.51

copper oxide, and subsequently, oxygen pressure leaching treatment was adopted.

3.2 Leaching test

The tailing residues after flotation is subjected to oxygen pressure leaching. In the autoclave, the components in the residue react with sulfuric acid to form soluble metal sulfates.[16] The reactions can be divided into four categories:

The first category is the reaction between salts such as silicates and acid, which can be expressed as:

$$2MeO\cdot SiO_2 + 2H_2SO_4 \rightarrow 2MeSO_4 + SiO_2 + 2H_2O \quad (1)$$

In the formula, Me represents Cu, Fe, Zn, Mo, *etc.*

The second category is the reaction between metal sulfides and acid, which can be expressed as:

$$MeS + 2O_2 \rightarrow 2MeSO_4 \quad (2)$$

The third category is the reaction between metal oxides and acid, which can be expressed as:

$$MeO + H_2SO_4 \rightarrow MeSO_4 + H_2O \quad (3)$$

The fourth category is the reaction between metallic elements in their elemental form and an acid, which can be expressed as:

$$Me + 1/2O_2 + H_2SO_4 \rightarrow MeSO_4 + H_2O \quad (4)$$

In a high-temperature and high-pressure environment, iron phases are acid-dissolved to form $FeSO_4$. Under oxygen-rich conditions, it is rapidly oxidized to $Fe_2(SO_4)_3$, which then undergoes a hydrolysis reaction to produce $FeSO_3$ and release sulfuric acid. The transformation of iron phases is closely related to the reaction temperature, oxygen partial pressure, and acid concentration, and the involved reactions are shown in the equations. Tromans' theory of oxygen solubility indicates that increasing the concentration of oxygen in the leaching solution can promote the oxidative dissolution of sulfides and enhance the oxidation and hydrolysis behavior of iron.[17] In order to improve the effect of oxygen pressure leaching, factors such as temperature, leaching time, sulfuric acid concentration, oxygen partial pressure, grinding fineness, and liquid–solid

Table 4 Copper phase analysis

Phase	Free copper oxide	Bonded copper oxide	Secondary copper sulfide	Primary copper sulfide	Total copper
Content (%)	0.03	0.066	0.16	0.004	0.26
Distribution rate (%)	11.54	25.38	61.54	1.54	100

ratio are selected to investigate their impacts on the leaching process.

3.2.1 Effect of sulfuric acid concentration. Under the conditions of a temperature of 200 °C, liquid–solid ratio of 8 mL g^{-1}, oxygen partial pressure of 700 kPa, particle size of −75 + 48 μm, and leaching time of 90 min, the influence of the sulfuric acid concentration on the leaching efficiency of Cu, Mo, and Fe in the slag sample is shown in Fig. 4(a). As shown in the figure, increasing the acidity can significantly increase the leaching efficiency of Cu and Mo. When the acidity reaches 0.35 mol L^{-1}, the leaching efficiency of Cu and Mo basically remains unchanged. The leaching rate of iron shows an upward trend with the increase of acidity. This is mainly because the increase in acidity will inhibit the hydrolysis of Fe^{3+} in the reaction kettle, thus increasing the leaching rate of iron. In the experiment, it was found that when the reaction acidity is high, the filtration time significantly increases. This is mainly due to the increased solubility of silicates, and the solution is also prone to generating silica gel and sol, which sharply deteriorates the filtration performance of the pulp. Therefore, considering comprehensively, the sulfuric acid concentration is selected as 0.35 mol L^{-1}. Finally, the leaching efficiency of Cu and Mo exceeds 95%, the leaching efficiency of iron is 13%, and the content of Cu in the leaching residue is lower than 0.03%.

3.2.2 Effect of temperature. Under the conditions of a sulfuric acid concentration of 0.35 mol L^{-1}, liquid–solid ratio of 8 mL g^{-1}, oxygen partial pressure of 700 kPa, particle size of −75 + 48 μm, and leaching time of 90 min, the temperature of the reaction kettle was controlled to explore the influence of the reaction temperature on the leaching efficiency of Cu, Mo, and Fe, as shown in the Fig. 4(b). It can be seen from the figure that with an increase in the reaction temperature, the leaching efficiency of Fe decreases significantly. When the temperature exceeds 200 °C, the leaching efficiency of Fe basically remains at around 10%. The leaching efficiency of Cu and Mo increases with the increase in temperature. This is mainly because the increase in temperature can promote the decomposition of copper phases, strengthen the hydrolysis of Fe^{3+} into hematite, and dehydrate silicic acid to produce insoluble SiO_2. Therefore, the leaching reaction temperature is selected as 200 °C. The leaching efficiencies of Cu and Mo are 96.31% and 94.78% respectively, and the leaching efficiency of iron is 10.77%.

3.2.3 Effect of oxygen partial pressure. Under the conditions of a sulfuric acid concentration of 0.35 mol L^{-1}, temperature of 200 °C, liquid–solid ratio of 8 mL g^{-1}, particle size of −75 + 48 μm, and leaching time of 90 min, the influence of the oxygen partial pressure on the leaching efficiency of Cu, Mo, and Fe is shown in Fig. 4(c). It can be seen from the figure that with the increase in the oxygen partial pressure, the leaching efficiency of Cu and Mo increases rapidly, along with a rapid decrease in the leaching efficiency of iron. This is mainly because increasing the oxygen partial pressure can increase the oxygen concentration in the leaching solution, promote the oxidative dissolution of sulfides, and enhance the oxidative hydrolysis of Fe. In order to improve the separation and recovery of Cu, Mo and Fe, the optimal oxygen partial pressure condition is 600 kPa.

3.2.4 Effect of the liquid–solid ratio. Under the conditions of a sulfuric acid concentration of 0.35 mol L^{-1}, temperature of 200 °C, oxygen partial pressure of 600 kPa, particle size of −75 + 48 μm, and leaching time of 90 min, the effect of the liquid–solid ratio on the leaching efficiency of Cu, Mo, and Fe is depicted in the Fig. 4(e). It is evident from the figure that as the liquid–solid ratio increases, the leaching efficiency of Cu and Mo rises, while the leaching efficiency of Fe declines. This is because an increase in the liquid–solid ratio can reduce the viscosity of the pulp, speed up molecular mass transfer, facilitate mineral dissolution, and enhance the hydrolysis of Fe^{3+}

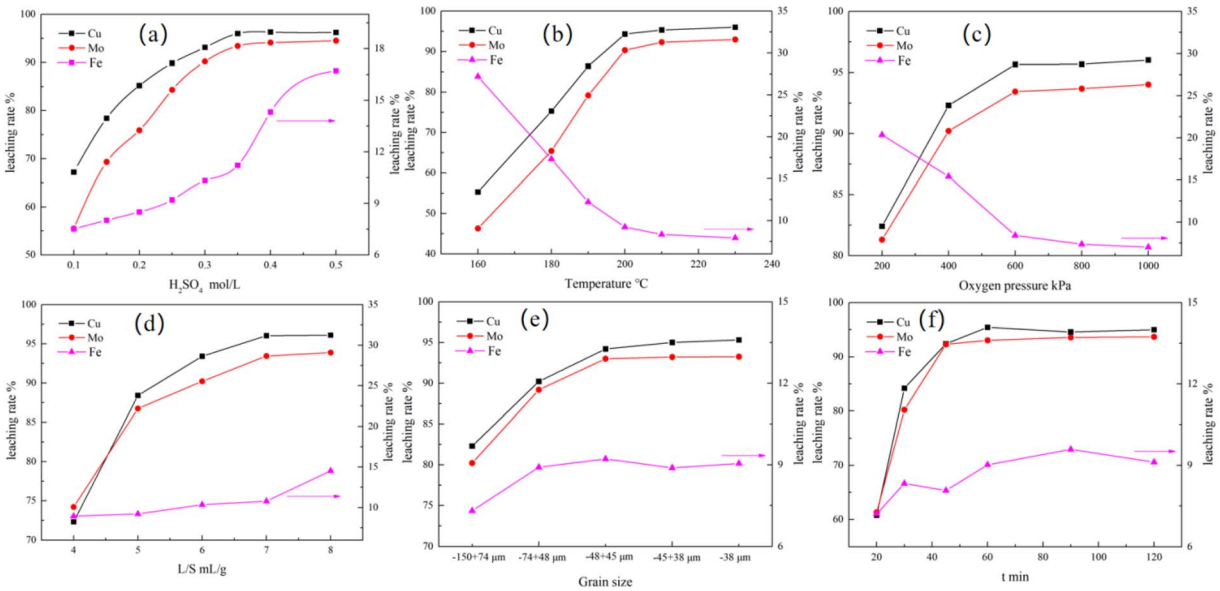

Fig. 4 Effect of leaching conditions on the leaching rate of copper: (a) sulfuric acid concentration, (b) leaching temperature, (c) oxygen pressure, (d) L/S ratio, (e) grain size, and (f) leaching time.

into Fe_2O_3. However, an increase in the liquid–solid ratio also leads to greater dissolution of silicates, which makes the subsequent filtration of the leaching solution more difficult. Therefore, after comprehensive consideration, a liquid–solid ratio of 7 mL g^{-1} is deemed more suitable.

3.2.5 Effect of particle size. Under the conditions where the sulfuric acid concentration is 0.35 mol L^{-1}, temperature is 200 °C, oxygen partial pressure is 600 kPa, liquid–solid ratio is 7 mL g^{-1}, and leaching time is 90 min, the impact of particle size on the leaching efficiency of Cu, Mo, and Fe is shown in the Fig. 4(f). It can be observed from the figure that the leaching efficiency of Cu, Mo, and Fe all increase rapidly as the particle size decreases. Once the particle size reaches −45 μm, the leaching efficiency basically remains constant. This is because when the particle size of the minerals decreases, the contact area between the minerals and the acid leaching solution increases to a certain extent. Meanwhile, the encapsulated Cu and Mo are liberated, thereby improving the leaching effect. Consequently, a particle size range of −45 + 38 μm is considered more appropriate.

3.2.6 Effect of leaching time. Under the conditions where the sulfuric acid concentration is 0.35 mol L^{-1}, temperature is 200 °C, oxygen partial pressure is 600 kPa, liquid–solid ratio is 7 mL g^{-1}, and particle size ranges from −45 to +38 μm, the impact of leaching time on the leaching efficiency of Cu, Mo, and Fe is presented in the Fig. 4(g). As can be seen from the figure, within the initial 45 minutes of the reaction, the leaching efficiency of metals Cu, Mo, and Fe essentially reaches a stable state. Taking all aspects into account, the reaction time is chosen to be 45 minutes.

3.3 Leaching kinetics analysis

3.3.1 Analysis of leaching kinetics control process. In the oxygen pressure acid leaching of flotation tailings, a complex solid–liquid–gas multiphase reaction system is established. The dissolution kinetics of mineral particles within this system are mainly dominated by three key factors. First, the diffusion of the leaching agent through the product layer plays a crucial role. Second, chemical reactions taking place on the surface of solid particles have a significant impact. Third, there is mixed control, which results from the synergistic effect of the above two mechanisms, as clearly illustrated in Fig. 5. To conduct an in-depth kinetic study of the oxygen pressure acid leaching process of the slag, the Shrinking Core Model (SCM) is applied.[18]

The rate equation of the Shrinking Core Model without Reaction (SCM) is as follows:[19,20]

$$1-(1-X)^{1/3}=\frac{k_c M_B C_A}{\alpha p_B r_0}=k_r t \quad (5)$$

$$1-\frac{2}{3}X-(1-X)^{2/3}=\frac{2M_B D_e C_A}{\alpha p_B r_0}t=k_d t \quad (6)$$

$$1-(1-X)^{1/3}-\frac{1}{3}\ln(1-X)=k_M\frac{C_A M_B}{p_B r_0}t \quad (7)$$

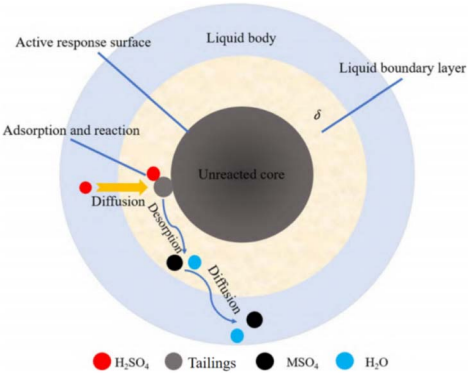

Fig. 5 Shrinkage model without the solid product layers of an unreacted nucleus.

Here, X is the leaching rate of the mineral element, %; M_B is the molar mass of the solute, g mol^{-1}; α is the stoichiometric coefficient of sulfuric acid in the reaction between the copper-containing compound and sulfuric acid; R_0 is the initial radius of the particle, μm; C_A is the concentration of the sulfuric acid solution, mol L^{-1}; D_e is the diffusion coefficient of the solid product layer, μm min^{-1}; ρ_B is the density of the particle, g cm^{-3}; t is the reaction time, min; k_r, k_d and k_M are the apparent rate constants, min^{-1}.

In order to determine the kinetic parameters and control mode of the oxygen pressure acid leaching, the Cu leaching rates at different temperatures were substituted into the formula for fitting, and the results are shown in Fig. 5(a)–(c), respectively. It can be seen from the figures that the early stage of the oxygen pressure leaching reaction fits well with eqn (5), and the later stage of the reaction fits well with eqn (6). The surface leaching process conforms to the unreacted shrinking core model. During the leaching process of Cu, it is first controlled by the chemical reaction and then by the diffusion of the solid product. The reaction rate constants k at different temperatures obtained by fitting are substituted into the Arrhenius equation:[21]

$$k=A\exp\left(\frac{-E_a}{RT}\right) \quad (8)$$

Here, A is the frequency factor; E_a is the apparent activation energy, kJ mol^{-1}; R is the gas equilibrium constant, $R = 8.314$ J mol^{-1}; T is the thermodynamic temperature, K.

The fitting results are shown in Fig. 5(d) and (e). According to the slope of the fitting equation, the apparent activation energies of the two-stage reactions are calculated to be 42.21 kJ mol^{-1} and 11.49 kJ mol^{-1}, respectively. The fitting results are within the ranges of the apparent activation energies for the chemical reaction control (>42 kJ mol^{-1}) and the diffusion control through the solid product layer (4–12 kJ mol^{-1}).[22] This further proves that the leaching of Cu in the mineral shifts from being controlled by the chemical reaction to being controlled by the diffusion of the solid product layer (Fig. 6).

3.3.2 Leaching kinetic equation. When the leaching time exceeds 50 min, the change in the metal leaching rate with time

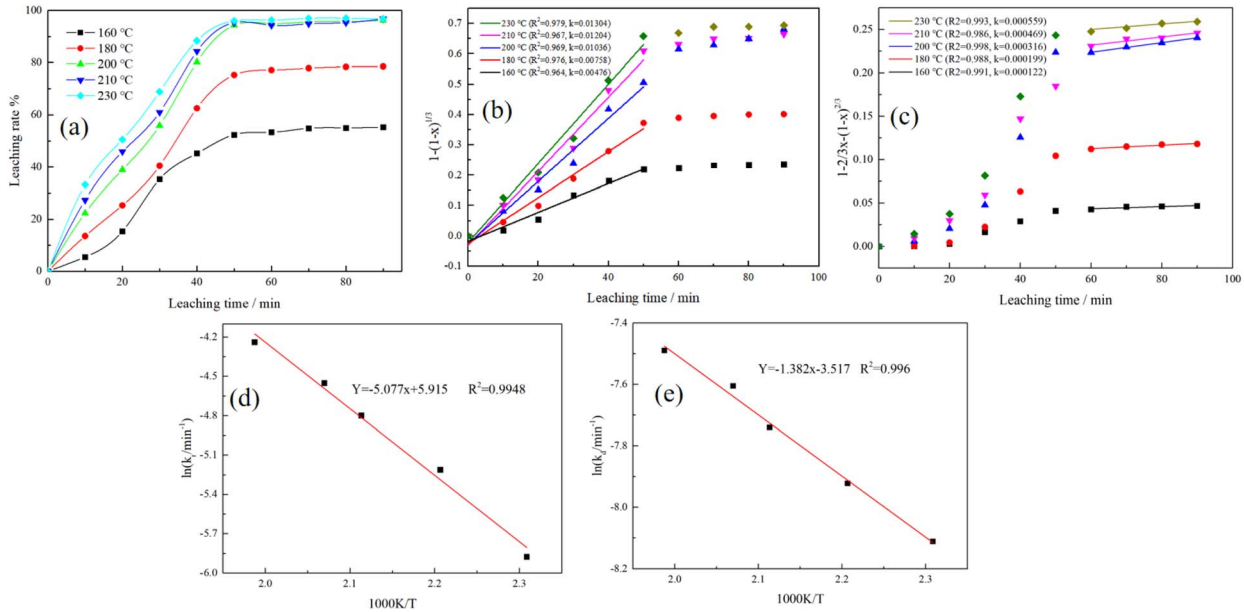

Fig. 6 (a) Effect of temperature on the leaching rate. (b) Relationship between $1-(1-x)^{1/3}$ and time (t) at different temperatures. (c) Relationship between $1-(2/3)x-(1-x)^{2/3}$ and time (t) at different temperatures. (d) Arrhenius equation fitting for chemically controlled stage. (e) Arrhenius equation fitting for diffusion-controlled stage.

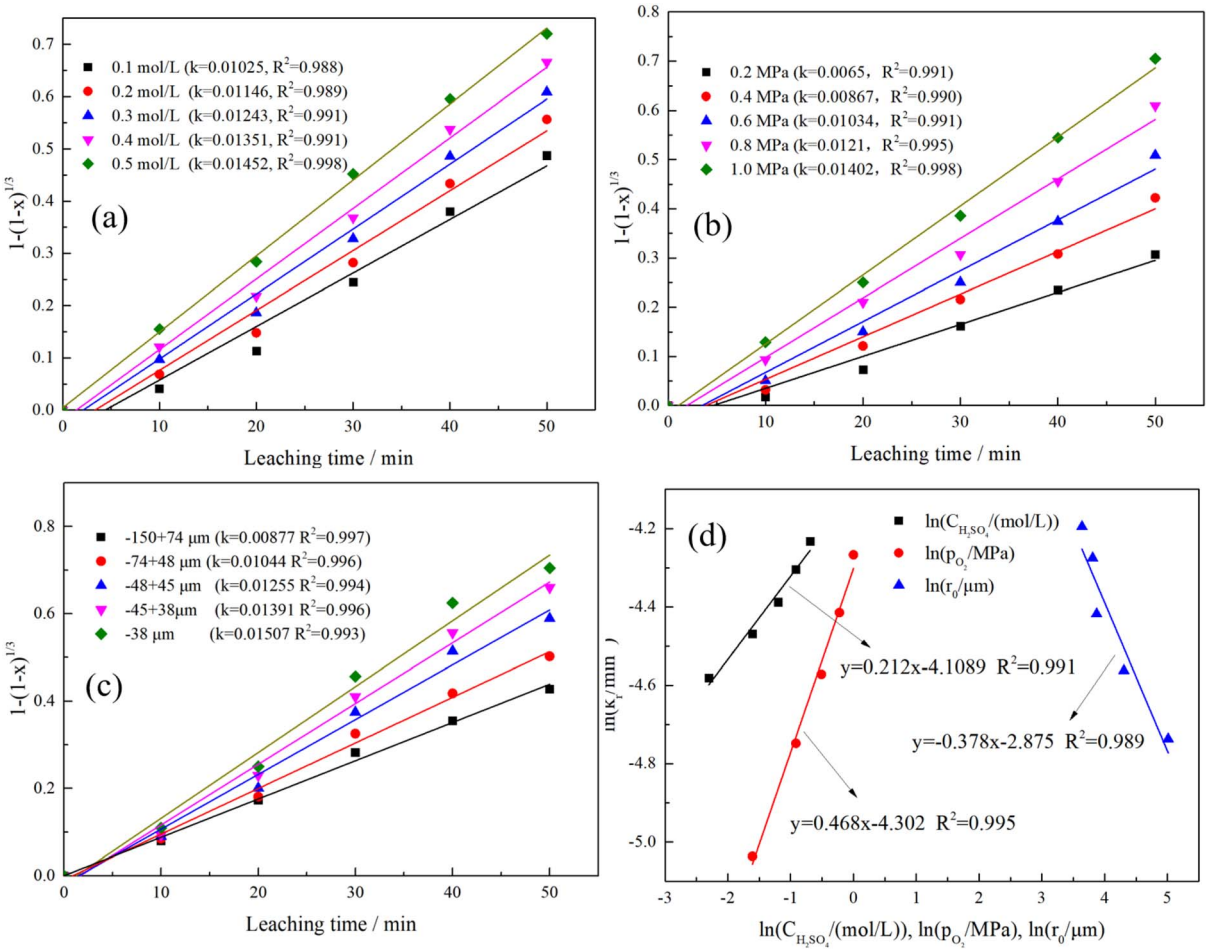

Fig. 7 Fitting results of the leaching rate of copper under different conditions: (a) sulfuric acid concentration, (b) oxygen partial pressure, and (c) particle size. (d) The fitting results of lnk with $\ln r_0$, $\ln C_{H_2SO_4}$ and $\ln p_{O_2}$.

is relatively small. The leaching process within 50 min is mainly controlled by chemical reactions, and the mixed control and diffusion control have little influence on the metal leaching rate. In the stage of chemical reaction control, the kinetic equation of oxygen pressure leaching can be expressed as eqn (9).

$$1-(1-X)^{1/3} = K_0 C_{H_2SO_4}{}^{n_1} P_{O_2}{}^{n_2} r_0{}^{n_3} e^{-\frac{E_a}{RT}} \quad (9)$$

Here, n_1, n_2, and n_3 are the reaction orders of the sulfuric acid concentration, oxygen partial pressure, and the initial radius of the material, respectively; K_0 is the rate constant related to temperature; $C_{H_2SO_4}$ is the sulfuric acid concentration, mol L^{-1}; p_{O_2} is the oxygen partial pressure, MPa.

Based on the leaching rates of Cu and Mo, plots were made by fitting $1-(1-x)^{1/3}$ against the leaching time. The fitting equations between different initial sulfuric acid concentrations, oxygen partial pressures, particle sizes, and $1-(1-x)^{1/3}$ were obtained. The results for Cu are shown in Fig. 7, and those for Mo are shown in Fig. 8. As can be seen from the figures, under different leaching time conditions, there is a good linear relationship between the experimental data of sulfuric acid concentration, oxygen partial pressure, particle size, and the leaching rates of Cu and Mo, and $1-(1-x)^{1/3}$. Then, plots were obtained by fitting the slope k_f of the straight-line against $\ln R_0$, $\ln C_{H_2SO_4}$, and $\ln p_{O_2}$, respectively. The slopes represent the reaction orders of sulfuric acid, oxygen partial pressure, and particle size. As can be seen from the figures, the parameters of sulfuric acid, oxygen partial pressure, and particle size in the reaction rate equation of Cu are 0.212, 0.468, and −0.378, respectively, while those in the reaction rate equation of Mo are 0.469, 0.506, and −0.435, respectively. On this basis, the values of K in the reaction equations of Cu and Mo were calculated to be 3.69×10^{-3} s^{-1} and 1.47×10^{-2} s^{-1}, respectively. Then, the kinetic equations for the oxygen-pressure leaching of Cu and Mo in the chemical reaction-controlled stage can be expressed as follows:

$$1-(1-X)^{1/3} = 3.69 \times 10^{-3} \cdot C_{H_2SO_4}{}^{0.212} P_{O_2}{}^{0.468} r_0{}^{-0.378} e^{-\frac{E_a}{RT}} t \quad (10)$$

$$1-(1-X)^{1/3} = 1.47 \times 10^{-2} \cdot C_{H_2SO_4}{}^{0.469} P_{O_2}{}^{0.506} r_0{}^{-0.435} e^{-\frac{E_a}{RT}} t \quad (11)$$

According to the experimental data and calculation results, the mechanism of action in the oxygen pressure leaching system was deduced from the core shrinkage model, as shown in Fig. 9. The specific description is as follows: (1) the leaching agent diffuses towards the surface of the particles through the diffusion layer; (2) the leaching agent diffuses into the solid

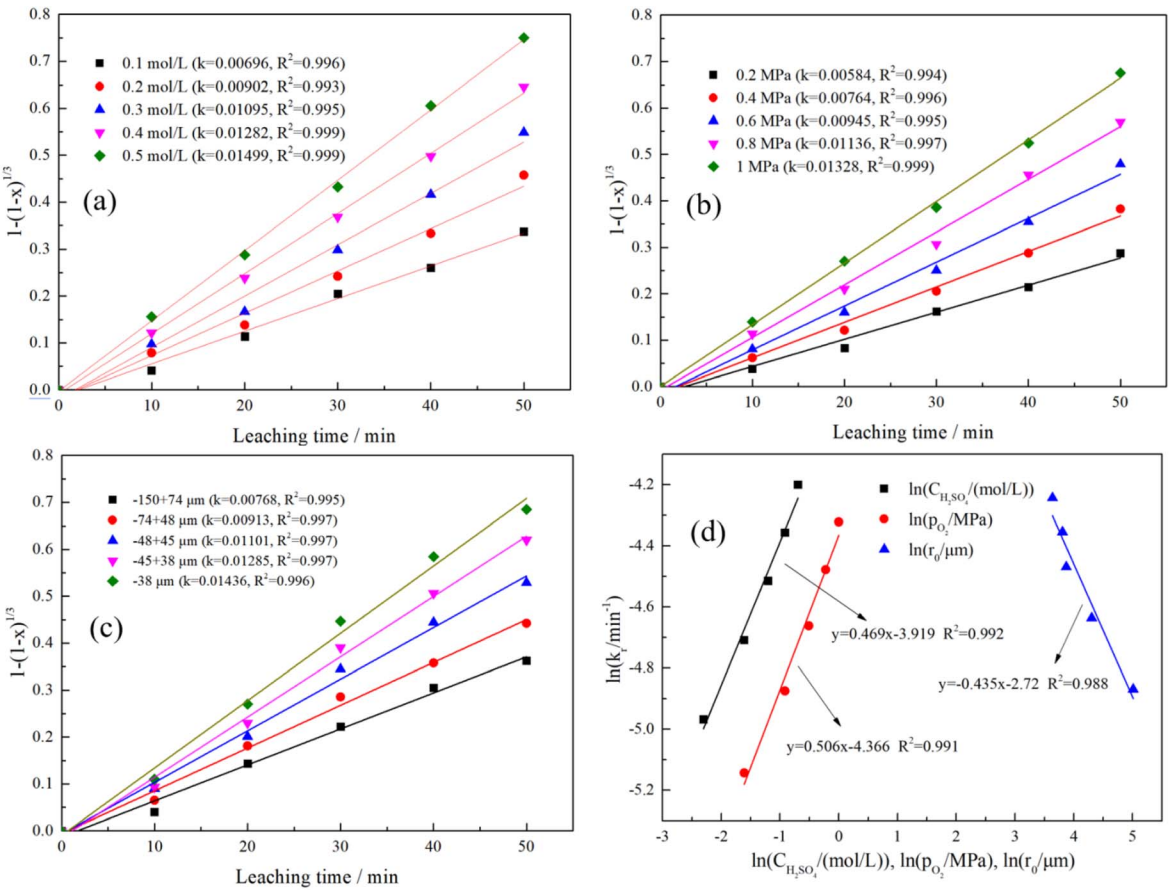

Fig. 8 Fitting results of the leaching rate of molybdenum under different conditions: (a) sulfuric acid concentration, (b) oxygen partial pressure, and (c) particle size. (d) The fitting results of $\ln k$ with $\ln r_0$, $\ln C_{H_2SO_4}$ and $\ln p_{O_2}$.

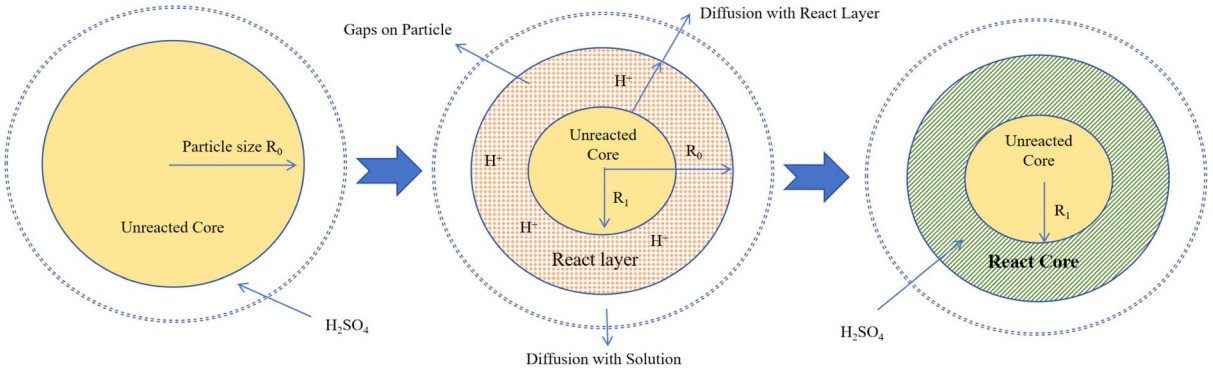

Fig. 9 Leaching process of copper and molybdenum in the oxygen pressure system.

membrane; (3) the leaching agent reacts with the mineral particles; (4) the insoluble products thicken the solid membrane and create voids, and the leaching agent permeates through the voids; (5) the soluble products diffuse into the leaching solution.

4 Conclusion

(1) For this copper smelting slag with a high oxidation rate, flotation is adopted to recover the easily separable copper sulfide minerals. Through a flotation process consisting of 1 roughing, 3 scavenging and 4 cleaning operations, the grade of the produced copper concentrate is 21.54%, and the recovery rate is 39.89%. The grade of Cu in the flotation tailings is 0.25%, and the content of Mo is 0.31%, which still has a relatively high recovery value.

(2) The tailings after flotation are subjected to oxygen pressure leaching to separately leach, separate and recover Cu, Mo and Fe. Under the conditions of a sulfuric acid concentration of 0.35 mol L^{-1}, a temperature of 200 °C, an oxygen partial pressure of 600 kPa, a liquid–solid ratio of 7 mL g^{-1}, a particle size of −45 + 38 μm and a leaching time of 45 min, the leaching rates of Cu and Mo are 96.87% and 95.39% respectively. Iron enters the slag phase, and the grade of Fe in the leaching slag is 62.76%, which can be used as a raw material for iron and steel smelting.

(3) The process of oxygen pressure acid leaching of Cu from flotation tailings conforms to the unreacted contracted core mode. In the early stage, it is controlled by the chemical reaction, then turns to the mixed-control stage, and in the later stage, it is controlled by the diffusion of the solid product layer. The apparent activation energies of the processes controlled by the chemical reaction and the diffusion of the solid product layer are 42.21 kJ mol^{-1} and 11.49 kJ mol^{-1}, respectively.

(4) The chemical reaction-controlled process is the main factor affecting the leaching of Cu and Mo. The reaction orders of the initial sulfuric acid concentration, oxygen partial pressure, and particle size are 0.212, 0.468, and −0.378, respectively. The kinetic equation for the leaching of Cu in the chemical reaction-controlled process is:

$$1-(1-X)^{1/3} = 3.69\times10^{-3}\cdot {C_{H_2SO_4}}^{0.212} {P_{O_2}}^{0.468} {r_0}^{-0.378} e^{-\frac{E_a}{RT}t}$$

The reaction orders of the initial sulfuric acid concentration, oxygen partial pressure, and particle size are 0.469, 0.506, and −0.435, respectively. The kinetic equation for the leaching of Mo in the chemical reaction-controlled process is:

$$1-(1-X)^{1/3} = 1.47\times10^{-2}\cdot {C_{H_2SO_4}}^{0.469} {P_{O_2}}^{0.506} {r_0}^{-0.435} e^{-\frac{E_a}{RT}t}$$

Author contributions

Zixuan Yang: investigation, Yuanlin Ma: data curation, Shuting Wang: writing – original draft, Tingtao Bi: funding acquisition.

Conflicts of interest

There are no known competing financial interests or personal relationships that could influence the publishing of this manuscript.

Data availability

All relevant data are within the paper.

Acknowledgements

Natural Science Foundation of Yunnan Province (no. 202501AU070075). Technology talent and platform plan (no. 202305AD160054).

References

1 B. Yang, D. Huang, D. Liu, *et al.*, Research and industrial application of a vacuum separation technique for recovering valuable metals from copper dross, *Sep. Purif. Technol.*, 2020, **236**(1), 116309.
2 L. Li, J. Peng, Z. Li, *et al.*, Synergistic inhibition effect of metal cations and tolyltriazole on copper in industrial cooling system, *Electrochim. Acta*, 2025, **522**(10), 145914.
3 Z. Qin, J. Xiao, J. Zhang, *et al.*, Practical experience to theoretical innovation: A model for recovering metal resources from industrial solid waste – A case study of

copper smelting slag, *Sep. Purif. Technol.*, 2025, **354**(7), 129395.

4 D. Chen, L. Hong, F. Nan, *et al.*, Heavy metals remediation through alkali assisted ball-milling activation of copper smelting slag for resource utilization, *J. Environ. Chem. Eng.*, 2024, **12**(3), 113053.

5 J. Sun, T. Zhang, P. Shen, *et al.*, Kinetics analysis of copper extraction from copper smelting slag by sulfuric acid oxidation leaching, *Miner. Eng.*, 2024, **216**, 108886.

6 Z. Qin, J. Xiao, T. Du, *et al.*, Resource utilization strategy of Fe-bearing smelting slag in China: A review Author links open overlay panel, *Miner. Eng.*, 2024, **219**, 109066.

7 J. Sun, L. Dong, T. Zhang, *et al.*, Efficient recovery of copper from copper smelting slag by gravity separation combined with flotation, *Chem. Eng. J.*, 2024, **494**(15), 153159.

8 P. Biernacka, M. Costas-Rodríguez, W. De Clercq, *et al.*, Capabilities and limitations of Pb, Sr and Fe isotopic analysis of iron-rich slags: a case study on the medieval port at Hoeke (Belgium), *RSC Adv.*, 2024, **14**(30), 21887–21900.

9 M. Fan and H. Liang, Soil health assessment of dressing and smelting slag field based on heavy metal pollution-buffer-fertility three aspects, *J. Hazard. Mater.*, 2025, **482**(15), 136602.

10 J. Shu, T. Lei, Y. Deng, *et al.*, Metal mobility and toxicity of reclaimed copper smelting fly ash and smelting slag, *RSC Adv.*, 2021, **11**(12), 6877–6884.

11 D. Dong and L. Yunhan, Processing of copper converter slag for metal reclamation. Part I: extraction and recovery of copper and cobalt, *Waste Manage. Res.*, 2007, **25**(5), 440–448.

12 F. Carranza, N. Iglesias and A. Mazuelos, *et a l.*, Ferric leaching of copper slag flotationtailings, *Miner. Eng.*, 2009, **22**, 107–110.

13 E. Rudnik, A. L. Burzyńsk and W. Gumowska, Hydrometallurgical recovery of copper and cobalt from reduction- roasted copper converter slag, *Miner. Eng.*, 2009, **22**(1), 88–95.

14 E. A. Vestola, M. K. Kuusenaho, H. M. Närhi, *et al.*, Acid bioleaching of solid waste materials from copper, steel and recycling industries, *Hydrometallurgy*, 2010, **103**(1–4), 74–79.

15 M. Baghalha, V. G. Papangelakis and K. W. Curlo, Factors affecting the leachability of Ni/Co/Cu slag sat hight emperature, *Hydrometallurgy*, 2007, **85**(1), 42–52.

16 F. Huang, Y. Liao, J. Zhou, *et al.*, Selective recovery of valua blemetals from nickel converter slag at elevated temperature with sulfuric acid solution, *Sep. Purif. Technol.*, 2015, **156**, 572–581.

17 D. Tromans, Oxygen solubility modeling in inorganic solutions: concentration, temperature and pressure effects, *Hydrometallurgy*, 1998, **50**(3), 279–296.

18 H. U. A. Yixin, *Introduction to Metallurgical Process dynamics [M]*, Metallurgical Industry Press, Beijing, 2004.

19 C. F. Dickinson and G. R. Heal, Solid – liquid diffusion controlled rate equations, *Thermochim. Acta*, 1999, **340–341**, 89–103.

20 (*a*) S. Aydogan, Dissolution kinetics of sphalerite with hydrogen peroxide in sulphuric acid medium, *Chem. Eng. J.*, 2006, **123**(3), 65–70; (*b*) K. Liu, Q. Y. Chen, Z. L. Yin, *et al.*, Kinetics of leaching of a Chinese laterite containing maghemite and magnetite in sulfuric acid solutions, *Hydrometallurgy*, 2012, **125**/**126**, 125–136.

21 M. Li, X. W. Zhang, Z. G. Liu, *et al.*, Kinetics of leaching fluoride from mixed rare earth concent rate with hydrochloric acid and aluminum chloride, *Hydrometallurgy*, 2013, **140**, 71–76.

22 G. X. He, Z. W. Zhao, X. B. Wang, *et al.*, Leaching kinetics of schee litein hydrochloric acid solution containing hydrogen peroxid e as complexing agent, *Hydrometallurgy*, 2014, **144**/**145**, 140–147.